

Strongly correlated system-reservoir dynamics with quantized pulses: Controlling the atom-photon bound state

Kisa Barkemeyer,* Andreas Knorr, and Alexander Carmele
Institut für Theoretische Physik, Technische Universität Berlin, 10623 Berlin, Germany

Within the matrix product state framework, we study the non-Markovian feedback dynamics of a two-level system interacting with the electromagnetic field inside a semi-infinite waveguide where the formation of an atom-photon bound state is possible. Taking the steady-state excitation of the emitter as a figure of merit, we compare the trapped excitation for an initially excited quantum emitter and an emitter prepared via quantized pulses. In the latter case, we find that for certain feedback delay times, multi-photon pulses yield a significantly higher steady-state excitation than possible with an initially excited emitter. In the system we consider, we find an increase of around 90 percent. Thus, the quantum optical initialization is found to be more efficient due to the self-consistent inclusion of emerging quantum noise. Furthermore, we propose a recursive Heisenberg ansatz which shows good qualitative agreement with the numerically expensive matrix product state method and requires only numerical resources growing quadratically with the number of excitations.

I. INTRODUCTION

A promising platform for a reliable implementation of large-scale quantum networks is offered by photonic quantum technologies where photons transport quantum information between the nodes of the network. The nodes, in turn, allow the storage as well as the manipulation of the information [1–10]. In recent years, special attention has been paid to waveguide quantum electrodynamics (w-QED) systems consisting of quantum few-level systems interacting with the electromagnetic field inside a one-dimensional waveguide. In these systems, enhanced light-matter interaction and interference effects can be observed due to the spatial confinement of the light field [11, 12]. This way, they allow for the creation of strong effective photon-photon interactions and qubit-qubit entanglement and, thus, are eligible candidates for the realization of quantum information processing protocols [13–17].

Such w-QED systems have been studied extensively in the Markovian regime where employed methods include the input-output formalism [12, 18–20], the Lippmann-Schwinger equation [15, 21, 22], a Green’s function approach [23, 24], as well as master equations [25, 26]. The Markovian approximation, however, breaks down if there is a macroscopical separation between the nodes compared to the wavelength of the light, for example, in long-distance networks. In this case, non-Markovian effects become important since the time-delayed backaction of the electromagnetic field on the emitters has to be taken into account. As a consequence, typical phenomena such as sub- and superradiance arise and the possibility to use time-delayed signals in the context of coherent feedback control is opened up [27–41]. An effective method to treat non-Markovian system dynamics is the matrix product state (MPS) framework [41–43] which allows the inclusion of quantized pulses [44].

A remarkable feature in w-QED systems is the formation of bound states in the continuum which can potentially be used for the storage of quantum information [45–53]. A paradigmatic setup in this regard is the two-level system (TLS) in

front of a mirror where emission properties depend sensitively on the emitter-mirror separation. Here, a finite excitation of the emitter in the long-time limit is possible due to the formation of an atom-photon bound state. This bound state can be populated by letting an initially excited emitter decay where it holds that the smaller the separation, the higher the steady-state excitation of the emitter [54, 55]. Another possibility to populate the bound state is via multi-photon pulses. In this case, the steady-state excitation depends non-monotonously on the emitter-mirror separation and for a fixed number of photons in the pulse, a certain minimum separation is required for the excitation scheme to work. Because of this non-monotonous behavior, studies with pulses containing variable numbers of photons are of interest for which an efficient description needs to be developed [56].

Here, we study the formation of an atom-photon bound state for a TLS inside a semi-infinite one-dimensional waveguide using the MPS framework for pulses containing up to $n = 3$ photons and look for ways to control and, in particular, maximize the steady-state excitation of the emitter. Although it is, in principle, possible to include higher photon numbers in the MPS framework, the numerical evaluation becomes increasingly expensive and a more efficient description becomes desirable. Therefore, we propose a formalism based on a recursion in the Heisenberg picture in which the interaction of quantum few-level systems with fully quantized multi-photon pulses in the non-Markovian regime can be approximated efficiently. Since the resources required for the numerical calculations only grow quadratically with the number of excitations, we can extend the investigation to $n = 15$ photons and more.

The paper is structured as follows: After this introduction in Sec. I, in Sec. II, we introduce the considered system and present the MPS method for the calculation of its dynamics including quantized pulses. The results we obtain this way are discussed in Sec. III. For an efficient estimation of the dynamics, in Sec. IV, we present our recursion method based on matrix elements in the Heisenberg picture. In Sec. V, the results it produces are presented after a comparison to the MPS results which allows an assessment of the validity of the approach. Finally, in Sec. VI, we summarize our findings.

* k.barkemeyer@tu-berlin.de

II. MPS METHOD

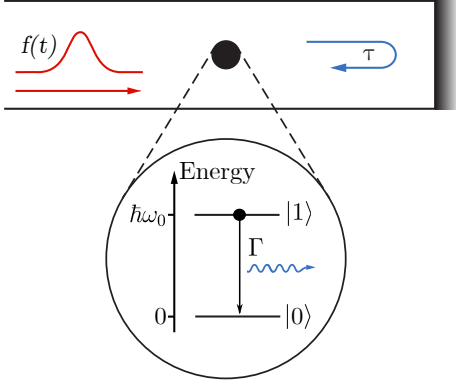


FIG. 1. TLS with transition frequency ω_0 and decay rate Γ inside a semi-infinite one-dimensional waveguide which provides feedback at the delay time τ . The TLS can be excited via a quantum pulse of shape $f(t)$.

Here, we present a method in the MPS framework which allows the numerically exact calculation of the dynamics in w-QED systems [42–44]. We use the approach to study the dynamics of a single TLS inside a semi-infinite waveguide. The closed end of the waveguide at a distance d from the TLS functions as a mirror. It feeds back the excitation emitted from the TLS after a delay time $\tau = 2d/c$ where c is the speed of light in the waveguide. The combined system of the TLS and the photonic reservoir is depicted in Fig. 1 and can be described via the Hamiltonian in dipole and rotating wave approximation

$$\mathcal{H} = \mathcal{H}_0 + \mathcal{H}_{\text{int}}, \quad (1)$$

$$\mathcal{H}_0 = \hbar\omega_0 E + \hbar \int d\omega \omega r_\omega^\dagger r_\omega, \quad (2)$$

$$\mathcal{H}_{\text{int}} = \hbar \int d\omega g(\omega) (r_\omega^\dagger \sigma_- + \text{H.c.}) \quad (3)$$

where ω_0 is the transition frequency of the TLS and the operator $E = \sigma_+ \sigma_-$ describes the occupation of its excited state. Its lowering (raising) operator is denoted by σ_- (σ_+) which, thus, can be interpreted as the polarization of the TLS and it holds that $\sigma_+ = \sigma_-^\dagger$. If we assume a single electron in the TLS we find $[\sigma_-, \sigma_+] = \mathbb{1} - 2E$. The annihilation (creation) of a photon with frequency ω in the reservoir is described by the bosonic operator $r_\omega^{(\dagger)}$. Reservoir and TLS are coupled with strength $g(\omega)$ which is, in general, frequency-dependent. Under the Markovian approximation, the coupling between the reservoir and the TLS can essentially be assumed as constant. Since we want to model feedback effects beyond the Markovian approximation, however, we consider a structured reservoir which results in the frequency-dependent coupling strength $g(\omega) = g_0 \sin(\omega\tau/2)$ where τ is the feedback-induced delay time.

We transform the Hamiltonian \mathcal{H} into the rotating frame

defined by its non-interacting part \mathcal{H}_0 which yields

$$\mathcal{H}' = \hbar \int d\omega g(\omega) (e^{i(\omega-\omega_0)t} r_\omega^\dagger \sigma_- + \text{H.c.}). \quad (4)$$

The Hamiltonian \mathcal{H}' governs the time evolution of the system which we discuss in the following section.

A. Time evolution

In this section, the time evolution method based on MPS is introduced in a condensed form to pave the way for the inclusion of quantized pulses. For a detailed derivation of the time evolution algorithm with feedback see Ref. [43]. The MPS framework is based on the Schrödinger picture. The main idea of the MPS time evolution method is to describe the continuous system dynamics via a stroboscopic time evolution at discrete time steps Δt which are small compared to the time scales of the system evolution. To start with, we introduce the time-dependent quantum noise operators [57]

$$r_t^\dagger = \frac{1}{\sqrt{2\pi}} \int d\omega r_\omega^\dagger e^{i(\omega-\omega_0)t}. \quad (5)$$

As the conjugate operators of r_t^\dagger , these collective operators describe the creation of a photon at time t and satisfy $[r_t, r_{t'}^\dagger] = \delta(t-t')$. With this definition, the Hamiltonian \mathcal{H}' from Eq. (4) can be written as

$$\mathcal{H}'(t) = -i\hbar \sqrt{\Gamma} [r_t^\dagger \sigma_- - r_{t-\tau}^\dagger \sigma_- e^{-i\omega_0\tau} - \text{H.c.}] \quad (6)$$

which is now explicitly time-dependent. Here, we defined the decay rate $\Gamma \equiv \pi g_0^2/2$. The first term on the right-hand side of Eq. (6) describes the immediate interaction of the TLS and the reservoir while the second term arises due to the feedback signal the effect of which is determined by the feedback phase $\phi \equiv \omega_0\tau$.

The dynamics of the system is governed by the Schrödinger equation

$$\frac{d}{dt} |\psi(t)\rangle = -\frac{i}{\hbar} \mathcal{H}'(t) |\psi(t)\rangle. \quad (7)$$

If we discretize time in sufficiently small steps Δt , the evolution from time t_k to t_{k+1} , $t_k = k\Delta t$, $k \in \mathbb{N}$, can be described via the stroboscopic time evolution operator U_k for which

$$|\psi(t_{k+1})\rangle = U_k |\psi(t_k)\rangle, \quad (8)$$

$$U_k = \exp\left[-\frac{i}{\hbar} \int_{t_k}^{t_{k+1}} dt' \mathcal{H}'(t')\right]. \quad (9)$$

Concretly, in our system, assuming $\tau = l\Delta t$, $l \in \mathbb{N}$, it takes the form

$$U_k = \exp\left[-\sqrt{\Gamma} \left[\Delta R^\dagger(t_k) \sigma_- - \Delta R^\dagger(t_{k-l}) \sigma_- e^{-i\omega_0\tau} - \text{H.c.} \right]\right] \quad (10)$$

where we defined the noise increments

$$\Delta R^\dagger(t_k) = \int_{t_k}^{t_{k+1}} dt r_t^\dagger. \quad (11)$$

These operators describe the creation of a photon in time step k and obey $[\Delta R(t_k), \Delta R^\dagger(t_{k'})] = \Delta t \delta_{kk'}$. With the noise increments, a discrete, orthonormal time-bin basis of the Hilbert space can be constructed since the Fock state describing the k -th time bin being occupied by i_k photons is obtained via

$$|i_k\rangle_k = \frac{[\Delta R^\dagger(t_k)]^{i_k}}{\sqrt{i_k! (\Delta t)^{i_k}}} |\text{vac}\rangle_k. \quad (12)$$

The general state of the TLS and the photonic reservoir in the time-bin basis takes the form

$$|\psi(t_k)\rangle = \sum_{i_1, \dots, i_{k-1}, i_S, i_k, \dots, i_N} \psi_{i_1, \dots, i_{k-1}, i_S, i_k, \dots, i_N} \times |i_1, \dots, i_{k-1}, i_S, i_k, \dots, i_N\rangle \quad (13)$$

where $i_S \in \{g, e\}$ denotes the TLS being either in the ground (g) or the excited state (e) while the index i_j , $j \in \{1, \dots, N\}$, describes the occupation of the j -th time bin. Time is assumed to run from t_1 to t_N . The coefficient tensor $\psi_{i_1, \dots, i_{k-1}, i_S, i_k, \dots, i_N}$ is, in general, $2p^N$ dimensional where $(p-1)$ is the maximum number of photons per time bin considered. The dimension of the Hilbert space, thus, grows exponentially with the number of time bins. To effectively reduce the dimension of the Hilbert space and enable an efficient numerical calculation of the dynamics, the coefficient tensor is decomposed into a product of matrices via a series of singular value decompositions. The state can subsequently be written as

$$|\psi(t_k)\rangle = \sum_{i_1, \dots, i_{k-1}, i_S, i_k, \dots, i_N} A^{i_1} \dots A^{i_{k-1}} A^{i_S} A^{i_k} \dots A^{i_N} \times |i_1, \dots, i_{k-1}, i_S, i_k, \dots, i_N\rangle. \quad (14)$$

This way, a time-local description is obtained since each matrix A^{i_j} refers to a specific time bin while the matrix A^{i_S} describes the TLS. Furthermore, the entanglement between the bins becomes accessible allowing a justified truncation of the least important parts of the Hilbert space.

The time evolution is eventually performed by contracting and decomposing the time evolution operator, the TLS bin, and the involved time bins where a swapping algorithm allows for the efficient inclusion of the non-Markovian feedback contributions.

B. Quantized pulses

Without a quantized pulse, that is, for a reservoir initially in the vacuum state, each of the time bins can be initialized in the vacuum state individually since the reservoir is found in a product state and there is no entanglement between the bins.

If we, however, drive the TLS with a quantized pulse, the involved reservoir bins become temporally entangled [44]. In

the case of a single-photon pulse, the initial state of the reservoir is given as

$$|\psi(t_0)\rangle_{\text{res}} = a_f^\dagger |0, \dots, 0\rangle \quad (15)$$

where a_f^\dagger is the creation operator of a wave packet with normalized pulse shape $f(t)$ for which [57]

$$a_f^\dagger = \int_{-\infty}^{\infty} dt f(t) r_t^\dagger, \quad \int_{-\infty}^{\infty} dt |f(t)|^2 = 1, \quad [a_f, a_f^\dagger] = 1. \quad (16)$$

For reasons of clarity, here, we focus on the state of the reservoir exclusively. Typically, the reservoir and the TLS are initially separable so that the TLS can be initialized independently. In the time-bin basis, assuming the pulse shape to be constant during one time step, that is, $f(t) = f_k$, $t \in [t_k, t_{k+1}[$, $k \in \{1, \dots, N\}$, the initial state is

$$|\psi(t_0)\rangle_{\text{res}} = \sum_{k=1}^N f_k \Delta R^\dagger(t_k) |0, \dots, 0\rangle. \quad (17)$$

A rectangular pulse which starts at $t_{\text{start}} = t_1$ and ends at $t_{\text{end}} = t_2$, for example, yields

$$\begin{aligned} |\psi(t_0)\rangle_{\text{res}} &= \frac{1}{\sqrt{2\Delta t}} [\Delta R^\dagger(t_1) + \Delta R^\dagger(t_2)] |0, \dots, 0\rangle \\ &= \frac{1}{\sqrt{2}} [|1, 0\rangle_{1,2} + |0, 1\rangle_{1,2}] \otimes |0, \dots, 0\rangle_{3, \dots, N} \end{aligned} \quad (18)$$

where the subscripts in the second line indicate the associated time bins. The time bins involved in the pulse cannot be initialized separately but due to their entanglement have to be initialized collectively and are subsequently decomposed into the MPS form.

To simulate n -photon pulses, we generalize the formalism accordingly to

$$|\psi(t_0)\rangle_{\text{res}} = \frac{1}{\sqrt{n!}} (a_f^\dagger)^n |0, \dots, 0\rangle \quad (19)$$

so that, for example, for $n = 2$ a pulse with the same shape as considered in Eq. (18) results in the initial state

$$\begin{aligned} |\psi(t_0)\rangle_{\text{res}} &= \frac{1}{\sqrt{4}} [|2, 0\rangle_{1,2} + |0, 2\rangle_{1,2} + \sqrt{2} |1, 1\rangle_{1,2}] \\ &\quad \otimes |0, \dots, 0\rangle_{3, \dots, N}. \end{aligned} \quad (20)$$

Although the MPS framework allows a numerically exact simulation of the system dynamics surpassing the common one- or two-photon limit, there are some drawbacks to the method. Namely, the method is limited to the few-photon case since the inclusion of excitations becomes increasingly expensive as discussed below in Sec. III. In addition to that, modeling pulses more complicated than the rectangular pulses we focused on so far is tedious since we have to perform costly series of singular value decompositions for the initialization of the reservoir state.

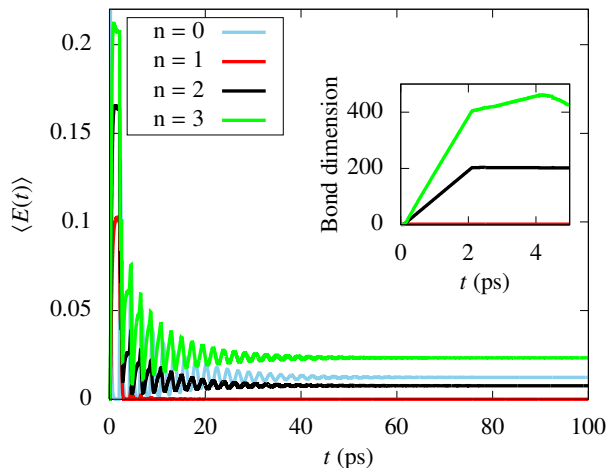


FIG. 2. Excitation of a TLS with decay rate $\Gamma = 4 \text{ ps}^{-1}$ subjected to feedback at $\tau = 2 \text{ ps}$ as a function of time. The TLS is either initially excited and decays in vacuum (light blue line), $n = 0$, or initially in the ground state and excited via a rectangular pulse of duration $t_p = 2.4 \text{ ps}$ which starts at $t_{\text{start}} = 0.1 \text{ ps}$ and contains n photons, $n \in \{1, 2, 3\}$ (red, black, and green line). Inset: Bond dimension of the time bins in the MPS implementation for an n -photon pulse.

III. CONTROLLING THE ATOM-PHOTON BOUND STATE

The formalism introduced above in Sec. II allows the simulation of the non-Markovian dynamics of quantum few-level systems driven via quantized pulses containing different numbers of photons. For the system we focus on, a TLS inside a semi-infinite waveguide, typical feedback effects such as the formation of a bound state in the continuum become possible. This phenomenon manifests as a stabilization of the excitation probability (henceforth termed excitation for brevity) of the TLS pointing to the formation of an atom-photon bound state [46].

Due to the implemented feedback mechanism, a signal emitted towards the mirror returns to the TLS after the delay time τ and interferes with the signal that is emitted from the TLS at that moment as illustrated in Fig. 1. The effect of the interference depends on the feedback phase $\varphi \equiv \omega_0 \tau$ where ω_0 is the transition frequency of the TLS. If the condition $\varphi = 2\pi m$, $m \in \mathbb{N}$, is met, the interference potentially leads to a stabilization of the excitation in the emitter and the trapping of a certain amount of excitation between the TLS and the mirror. For a feedback phase $\varphi \neq 2\pi m$, in the long-time limit, the emitter inevitably decays to the ground state [53, 58]. Henceforth, we assume that a feedback phase $\varphi = 2\pi m$ is implemented so that the formation of an atom-photon bound state is, in principle, possible. In our analysis, we concentrate on the steady-state excitation of the emitter, that is, the excitonic component of the atom-photon bound state, as a measure of the excitation trapping.

The dynamics of the excitation of a TLS with decay rate $\Gamma = 4 \text{ ps}^{-1}$ subjected to feedback at delay time $\tau = 2 \text{ ps}$ is

shown in Fig. 2 where specific parameter values are chosen out of numerical convenience. The calculations were performed using the ITensor library [59]. Since $\Gamma\tau \gg 1$, here, we operate in the strongly non-Markovian regime. There are different scenarios in which an atom-photon bound state is formed: On the one hand, a stabilization of the excitation can be observed for an initially excited emitter which does not fully decay in vacuum (light blue line). In this case, the amount of excitation trapped in the system decays monotonously with $\Gamma\tau$ [54]. On the other hand, we can evoke a stabilization of the excitation in a TLS that is initially in the ground state using multi-photon pulses. In this case, the shape of the pulse and the contained number of photons additionally influence the trapped excitation. In Fig. 2, a rectangular pulse of duration $t_p = 2.4 \text{ ps}$ containing either one, two, or three photons is considered. For a TLS initially in the ground state, a single-photon pulse does not cause a stabilization at a finite amount of excitation (red line). We need at least two photons in the pulse to evoke such behavior where the first photon partially excites the emitter and due to the scattering of the remaining photons a non-zero steady state can be reached [56]. This occurs for the two-photon pulse (black line); a three-photon pulse, however, leads to an even higher steady-state excitation for the system under consideration (green line). We are interested in ways to control and, in particular, maximize the excitation trapping. Therefore, we note that the steady-state excitation of the TLS presented in Fig. 2 for a rectangular three-photon pulse ($\langle E(t_\infty) \rangle \equiv \lim_{t \rightarrow \infty} \langle E(t) \rangle = 0.0234$) exceeds the excitation at which the initially excited TLS in vacuum stabilizes ($\langle E(t_\infty) \rangle = 0.0124$). This corresponds to an increase of around 90 percent. Thus, our findings suggest that the quantum optical preparation of an excited emitter via multi-photon pulses can be significantly more effective than via an initially excited emitter due to the self-consistent inclusion of quantum noise.

In the inset of Fig. 2, the bond dimension of the time bins in the MPS implementation for different numbers of photons and a TLS initially in the ground state is shown. The bond dimension of the time bins quantifies their entanglement and, hence, functions as a measure of the required computational resources. In case of a single-photon pulse, the maximum is reached at $t = t_{\text{start}}$ where the pulse starts. For a two-photon pulse, in contrast, the bond dimension reaches its maximum around the time when the first feedback signal returns to the emitter, that is, at $t = t_{\text{start}} + \tau$. In case of a three-photon pulse, after two feedback intervals, at $t = t_{\text{start}} + 2\tau$, the bond dimension takes on its maximum before decaying again. The significant increase of the maximum bond dimension illustrates the unfavorable scaling of the MPS method with the number of excitations. To enable the inclusion of higher numbers of photons, it is, thus, reasonable to look for approximate methods scaling more advantageously.

IV. RECURSIVE HEISENBERG METHOD

To efficiently estimate the dynamics for the TLS subjected to quantized pulses and non-Markovian feedback, we employ

a method based on the Heisenberg picture. Using the Hamiltonian \mathcal{H}' from Eq. (4), we derive differential equations for the operators $E(t)$, $\sigma_-(t)$, and $r_\omega(t)$ which are time-dependent in the Heisenberg picture. An arbitrary Heisenberg operator $A(t)$ is related to its counterpart in the Schrödinger picture $A_S = A(0)$ via

$$A(t) = U^\dagger(t, 0) A_S U(t, 0) \quad (21)$$

where $U(t, 0)$ is the time-evolution operator from time 0 to time t . Assuming no explicit time dependence, $A(t)$ obeys the Heisenberg equation of motion

$$\frac{d}{dt} A(t) = \frac{i}{\hbar} U^\dagger(t, 0) [\mathcal{H}', A_S] U(t, 0). \quad (22)$$

This way, we obtain

$$\frac{d}{dt} E(t) = i \int d\omega g(\omega) \left[e^{i(\omega-\omega_0)t} r_\omega^\dagger(t) \sigma_-(t) - \text{H.c.} \right], \quad (23)$$

$$\frac{d}{dt} \sigma_-(t) = -i \int d\omega g(\omega) e^{-i(\omega-\omega_0)t} [\mathbb{1} - 2E(t)] r_\omega(t), \quad (24)$$

$$\frac{d}{dt} r_\omega(t) = -ig(\omega) e^{i(\omega-\omega_0)t} \sigma_-(t). \quad (25)$$

We integrate out the reservoir modes by formally integrating Eq. (25) and plugging the result

$$r_\omega(t) = r_\omega(0) - ig(\omega) \int_0^t dt' e^{i(\omega-\omega_0)t'} \sigma_-(t') \quad (26)$$

into Eqs. (23) and (24). In analogy to the MPS method presented in Sec. II, we introduce the quantum noise operators $r_i^\dagger(0)$ as the conjugate operators of $r_\omega^\dagger(0)$ [see Eq. (5)] which allow the description of a fully quantized input pulse [60, 61]. The Markovian case where we assume a constant coupling strength between the emitter and the reservoir has been discussed extensively in the literature [18, 20, 62, 63]. If a feedback mechanism at delay time $\tau > 0$ is implemented, we assume a sinusoidal frequency dependence of the coupling strength, $g(\omega) = g_0 \sin(\omega\tau/2)$, and define the delayed input operator

$$r_{i,\tau}^\dagger \equiv r_{i-\frac{\tau}{2}}^\dagger(0) e^{-i\omega_0\frac{\tau}{2}} - r_{i+\frac{\tau}{2}}^\dagger(0) e^{i\omega_0\frac{\tau}{2}}. \quad (27)$$

This way, Eqs. (23) and (24) in the case of non-Markovian dynamics yield the delay differential equations [64]

$$\begin{aligned} \frac{d}{dt} E(t) = & -2\Gamma E(t) - \sqrt{\Gamma} \left[r_{i,\tau}^\dagger \sigma_-(t) + \text{H.c.} \right] \\ & + \Gamma \left[e^{-i\omega_0\tau} \sigma_+(t-\tau) \sigma_-(t) + \text{H.c.} \right] \Theta(t-\tau), \end{aligned} \quad (28)$$

$$\begin{aligned} \frac{d}{dt} \sigma_-(t) = & -\Gamma \sigma_-(t) - \sqrt{\Gamma} [\mathbb{1} - 2E(t)] r_{i,\tau} \\ & + \Gamma e^{i\omega_0\tau} [\sigma_-(t-\tau) - 2E(t) \sigma_-(t-\tau)] \Theta(t-\tau) \end{aligned} \quad (29)$$

where we again used the definition of the decay rate $\Gamma = \pi g_0^2/2$ and find that after the non-negligible delay time τ , feedback effects influence the dynamics.

The combined state of the TLS and the reservoir is of the form $|j, n\rangle$ where $j \in \{g, e\}$ denotes the TLS being either in the

ground (g) or the excited state (e) while $n \in \mathbb{N}$ indicates the number of photons in the reservoir. Like introduced for the MPS method, the n -photon state can be constructed via

$$|j, n\rangle = \frac{1}{\sqrt{n!}} (a_f^\dagger)^n |j, 0\rangle \quad (30)$$

where a_f^\dagger is the creation operator of a wave packet of shape $f(t)$ with the properties given in Eq. (16). Conversely, the annihilation of a photon can be described as

$$r_i |j, n\rangle = \begin{cases} 0, & n = 0 \\ \sqrt{n} f(t) |j, n-1\rangle, & n > 0 \end{cases}. \quad (31)$$

As for the MPS method, we assume the TLS and the reservoir to be initially separable so that we can calculate the expectation value of the occupation operator of the TLS, $\langle E(t) \rangle = \langle \psi(0) | E(t) | \psi(0) \rangle$, using an initial state of the above form, so that $|\psi(0)\rangle = |j, n\rangle$. When calculating this expectation value numerically using Eq. (28), we find a coupling to matrix elements which obey

$$\begin{aligned} \frac{d}{dt} \langle i, m | E(t) | k, p \rangle = & -2\Gamma \langle i, m | E(t) | k, p \rangle \\ & - \sqrt{\Gamma} \left[\langle i, m | r_{i,\tau}^\dagger \sigma_-(t) | k, p \rangle + \langle i, m | \sigma_+(t) r_{i,\tau} | k, p \rangle \right] \\ & + \Gamma \left[e^{-i\omega_0\tau} \langle i, m | \sigma_+(t-\tau) \sigma_-(t) | k, p \rangle \right. \\ & \left. + e^{i\omega_0\tau} \langle i, m | \sigma_+(t) \sigma_-(t-\tau) | k, p \rangle \right] \Theta(t-\tau), \end{aligned} \quad (32)$$

$$\begin{aligned} \frac{d}{dt} \langle i, m | \sigma_-(t) | k, p \rangle = & -\Gamma \langle i, m | \sigma_-(t) | k, p \rangle \\ & - \sqrt{\Gamma} \left[\langle i, m | r_{i,\tau} | k, p \rangle - 2 \langle i, m | E(t) r_{i,\tau} | k, p \rangle \right] \\ & + \Gamma e^{i\omega_0\tau} \left[\langle i, m | \sigma_-(t-\tau) | k, p \rangle \right. \\ & \left. - 2 \langle i, m | E(t) \sigma_-(t-\tau) | k, p \rangle \right] \Theta(t-\tau). \end{aligned} \quad (33)$$

For a system with feedback, the time-delayed terms in Eqs. (32) and (33) become relevant and a hierarchy problem occurs due to the two-time correlations in the last two lines of Eq. (32) and the last line of Eq. (33). To avoid the explicit calculation of the two-time correlations with time-ordering in the Heisenberg picture, we make the ansatz to unravel these terms via the insertion of a unity

$$\mathbb{1} = \sum_{\substack{l=q, e \\ q=0, 1, \dots}} |l, q\rangle \langle l, q| \quad (34)$$

between the operators with different time arguments. This way, we shift the problem to the calculation of the matrix elements of single time Heisenberg operators. We recursively insert the results from Eqs. (32) and (33) to evaluate the two-time correlations and close the set of differential equations. This efficient recursive approach only keeps track of the non-Markovian quantum noise partially, see Sec. V, but accelerates the calculations by orders of magnitude.

For certain setups such as the TLS in front of a mirror, it is sufficient to consider a maximum number of $q = n$ photons for a TLS subjected to a pulse containing n photons, $n \in \mathbb{N}$, since

matrix elements with higher photon numbers do not couple to the dynamics. Within our assumption, we can, therefore, evaluate the respective terms according to

$$\langle i, m | \sigma_+(t - \tau) \sigma_-(t) | k, p \rangle = \sum_{\substack{l=g,e \\ q=0,1,\dots,n}} \langle i, m | \sigma_+(t - \tau) | l, q \rangle \langle l, q | \sigma_-(t) | k, p \rangle, \quad (35)$$

$$\langle i, m | E(t) \sigma_-(t - \tau) | k, p \rangle = \sum_{\substack{l=g,e \\ q=0,1,\dots,n}} \langle i, m | E(t) | l, q \rangle \langle l, q | \sigma_-(t - \tau) | k, p \rangle. \quad (36)$$

If we consider an n -photon pulse, we have to calculate and save $4(n + 1)^2$ matrix elements for the full dynamics in each timestep. Thus, an efficient estimation of the non-Markovian dynamics is possible since the required computation time and memory only grow quadratically with the number of excitations. In the following section, we study the range of validity of our approximation.

V. EFFICIENT ESTIMATION OF THE DYNAMICS

After the introduction of the Heisenberg method, in this section, we study its applicability by comparing the results it produces with the results obtained using the MPS method. Subsequently, we employ the recursive Heisenberg method for qualitatively exploring regions in parameter space previously inaccessible due to computational limitations.

A. Comparison with MPS results

For an infinite waveguide, that is, without feedback, the time-delayed terms in Eqs. (32) and (33) can be omitted. In this case, we can evaluate the matrix elements without any approximations so that the Heisenberg method produces numerically exact results which agree perfectly with the MPS results (not shown). In this regime, the Heisenberg approach clearly outperforms the MPS method due to its advantageous scaling.

With feedback, however, the time-delayed terms have to be taken into account so that the system of differential equations does not close trivially. The impact of the ansatz we use to approach this problem [see Eq. (34)] depends on the number of excitations in the system. This is illustrated in Fig. 3 by the example of a TLS with decay rate $\Gamma = 4 \text{ ps}^{-1}$ subjected to feedback at $\tau = 2 \text{ ps}$ which is driven via rectangular pulses of duration $t_p = 2.4 \text{ ps}$ containing different numbers of photons. Note that the system is the same as the one considered for Fig. 2. If we restrict the dynamics to the single-excitation subspace, the results agree with those obtained with the MPS method: For a TLS initially in the ground state subjected to a single-photon pulse, the results coincide perfectly (Inset). The same applies for a TLS initially in the excited state without an additional pulse (not shown). Beyond the single-excitation manifold, quantitative deviations of the Heisenberg results from those

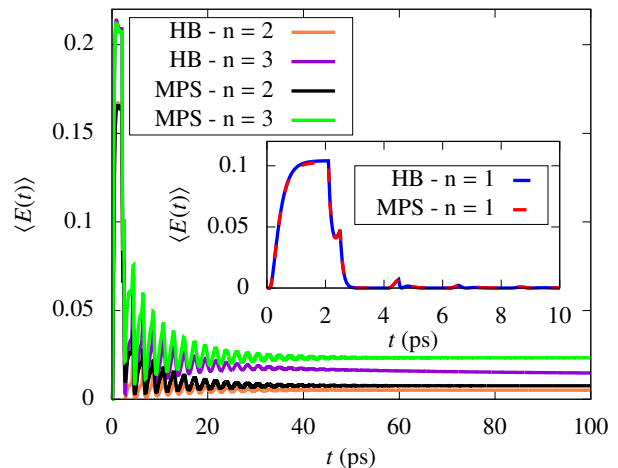


FIG. 3. Comparison of the results using the MPS and the Heisenberg (HB) method for the dynamics of the excitation of a TLS with decay rate $\Gamma = 4 \text{ ps}^{-1}$ subjected to feedback at $\tau = 2 \text{ ps}$. The TLS is initially in the ground state and excited via a rectangular pulse of duration $t_p = 2.4 \text{ ps}$ which starts at $t_{\text{start}} = 0.1 \text{ ps}$ and contains n photons, $n \in \{2, 3\}$. Inset: Comparison for a single-photon pulse where $n = 1$.

produced via the MPS method arise (orange and black line for two, violet and green line for three photons) which we relate to an underestimation of quantum correlations between the emitter and the reservoir. Nevertheless, qualitatively, the Heisenberg method captures the dynamics and the results show good agreement. This works particularly well in the strongly non-Markovian regime where $\Gamma\tau \gg 1$. In conclusion, the Heisenberg method is suitable for an efficient qualitative estimation of the essential system dynamics due to its favorable scaling.

B. Newly accessible regions in parameter space

With the Heisenberg method, we are able to estimate the interaction of a TLS subjected to non-Markovian feedback with pulses of various pulse shapes containing numbers of photons exceeding the limit of one, two, or three photons by lengths since the required computational resources only grow quadratically with the number of photons in the pulse. Although the results are quantitatively not exact, they allow a beneficial qualitative approximation of the system dynamics and, in particular, the prediction of atom-photon bound states.

We can, for example, use the method to determine the number of photons needed to excite a bound state for a given $\Gamma\tau$ as well as to find the number of photons that maximizes the steady-state excitation for a particular pulse shape. In Fig. 4, the estimated steady-state excitation for a TLS driven via a Gaussian pulse ($f(t) = A \exp[-(t - \mu)^2 / (2\sigma^2)]$) with normalization constant A , width $\sigma = 7 \text{ ps}$, and offset μ containing different numbers of photons as a function of $\Gamma\tau$ is shown. In the case of an initially excited TLS, it holds that the smaller $\Gamma\tau$, the more excitation is trapped. For the excitation of a TLS via a multi-photon pulse, in contrast, a certain $\Gamma\tau$ is neces-

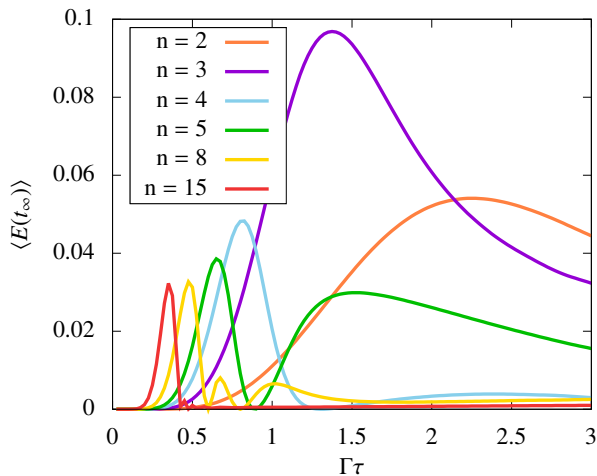


FIG. 4. Steady-state excitation of a TLS subjected to feedback and a Gaussian pulse with width $\sigma = 7$ ps containing n photons as a function of $\Gamma\tau$ estimated using the Heisenberg method.

sary for the excitation scheme to work. We observe that the smaller $\Gamma\tau$, the higher the number of photons that is needed so that a non-trivial steady-state can be reached. Furthermore, we find that the smaller $\Gamma\tau$, the higher the number of photons which yields the highest possible steady-state excitation. For the pulse shape under consideration, the highest value can be obtained with three photons at $\Gamma\tau = 1.375$ with an estimated value of $\langle E(t_{\infty}) \rangle = 0.097$.

VI. CONCLUSION AND OUTLOOK

We studied the interaction of a TLS with the electromagnetic field inside a semi-infinite one-dimensional waveguide within the MPS framework. In this system, multi-photon pulses can induce an atom-photon bound state. Our analysis for up to $n = 3$ photons showed that, this way, it is possible to stabilize the emitter at a steady-state excitation exceeding that of an initially excited TLS decaying in vacuum significantly.

In the system we considered, we found an increase of around 90 percent. This shows that multi-photon pulses are a versatile tool for the control of the atom-photon bound state and we conclude that the quantum optical preparation of an excited emitter via multi-photon pulses can be more efficient than the semiclassical preparation with an initially excited emitter due to the self-consistent treatment of quantum noise.

To overcome numerical limitations we introduced a recursive method based on the Heisenberg picture which allows the efficient estimation of the non-Markovian feedback dynamics for quantum few-level systems subjected to multi-photon pulses. The required computational resources grow quadratically with the number of photons in the pulse, thus, making it possible to surpass the usual few-photon limit. In addition to that, the approach simplifies the consideration of arbitrary pulse shapes. We employed the method to study the influence of pulses containing up to $n = 15$ photons on the TLS dynamics. This way, we were able to study the non-monotonous dependence of the steady-state excitation on the emitter-mirror separation and found that the smaller the separation, the more photons are needed to induce an atom-photon bound state. Furthermore, the smaller the separation the higher the number of photons that results in the highest possible steady-state excitation. Thus, the findings suggest that it is possible to realize tailored trapping scenarios using pulse engineering which can be an important step on the path towards the implementation of effective quantum memory.

It will be interesting to extend our model to more complex systems consisting of multiple emitters where, for example, the effect of quantum pulses on the entanglement of the emitters can be studied.

ACKNOWLEDGEMENTS

The authors gratefully acknowledge the support of the Deutsche Forschungsgemeinschaft (DFG) through the project B1 of the SFB 910 and from the European Unions Horizon 2020 research and innovation program under the SONAR grant Agreement No.734690.

-
- [1] J. I. Cirac, P. Zoller, H. J. Kimble, and H. Mabuchi, *Phys. Rev. Lett.* **78**, 3221 (1997).
 - [2] A. S. Parkins and H. J. Kimble, *J. Opt. B* **1**, 496 (1999).
 - [3] D. P. DiVincenzo, *Fortschritte der Phys.* **48**, 771 (2000).
 - [4] E. Knill, R. Laflamme, and G. J. Milburn, *Nature* **409**, 46 (2001).
 - [5] P. Zoller, T. Beth, D. Binosi, R. Blatt, H. Briegel, D. Bruss, T. Calarco, J. I. Cirac, D. Deutsch, J. Eisert, A. Ekert, C. Fabre, N. Gisin, P. Grangiere, M. Grassl, S. Haroche, A. Imamoglu, A. Karlson, J. Kempe, L. Kouwenhoven, S. Kröll, G. Leuchs, M. Lewenstein, D. Loss, N. Lütkenhaus, S. Massar, J. E. Mooij, M. B. Plenio, E. Polzik, S. Popescu, G. Rempe, A. Sergienko, D. Suter, J. Twamley, G. Wendin, R. Werner, A. Winter, J. Wrachtrup, and A. Zeilinger, *Eur. Phys. J. D* **36**, 203 (2005).
 - [6] H. J. Kimble, *Nature* **453**, 1023 (2008).
 - [7] J. L. O'Brien, A. Furusawa, and J. Vučković, *Nat. Photonics* **3**, 687 (2009).
 - [8] M. A. Nielsen and I. L. Chuang, *Quantum Computation and Quantum Information* (Cambridge University Press, Cambridge, 2010).
 - [9] T. E. Northup and R. Blatt, *Nat. Photonics* **8**, 356 (2014).
 - [10] B. Vermersch, P. O. Guimond, H. Pichler, and P. Zoller, *Phys. Rev. Lett.* **118**, 133601 (2017).
 - [11] D. E. Chang, A. S. Sørensen, P. R. Hemmer, and M. D. Lukin, *Phys. Rev. Lett.* **97**, 053002 (2006).
 - [12] S. Fan, Ş. E. Kocabaş, and J. T. Shen, *Phys. Rev. A* **82**, 063821 (2010).

- [13] D. E. Chang, A. S. Sørensen, E. A. Demler, and M. D. Lukin, *Nat. Phys.* **3**, 807 (2007).
- [14] F. Ciccarello, D. E. Browne, L. C. Kwek, H. Schomerus, M. Zarcone, and S. Bose, *Phys. Rev. A* **85**, 050305 (2012).
- [15] H. Zheng and H. U. Baranger, *Phys. Rev. Lett.* **110**, 113601 (2013).
- [16] H. Zheng, D. J. Gauthier, and H. U. Baranger, *Phys. Rev. Lett.* **111**, 090502 (2013).
- [17] C. Gonzalez-Ballester, E. Moreno, and F. J. Garcia-Vidal, *Phys. Rev. A* **89**, 042328 (2014).
- [18] A. H. Kiilerich and K. Mølmer, *Phys. Rev. Lett.* **123**, 123604 (2019).
- [19] A. H. Kiilerich and K. Mølmer, *Phys. Rev. A* **102**, 023717 (2020).
- [20] Z. Liao, Y. Lu, and M. S. Zubairy, *Phys. Rev. A* **102**, 053702 (2020).
- [21] J. T. Shen and S. Fan, *Phys. Rev. A* **76**, 062709 (2007).
- [22] Y.-L. L. Fang, H. Zheng, and H. U. Baranger, *EPJ Quantum Technol.* **1**, 3 (2014).
- [23] D. Dzsoťjan, A. S. Sørensen, and M. Fleischhauer, *Phys. Rev. B* **82**, 075427 (2010).
- [24] M. P. Schneider, T. Sproll, C. Stawiarski, P. Schmitteckert, and K. Busch, *Phys. Rev. A* **93**, 013828 (2016).
- [25] B. Q. Baragiola, R. L. Cook, A. M. Brańczyk, and J. Combes, *Phys. Rev. A* **86**, 013811 (2012).
- [26] D. E. Chang, L. Jiang, A. V. Gorshkov, and H. J. Kimble, *New J. Phys.* **14**, 063003 (2012).
- [27] H. M. Wiseman and G. J. Milburn, *Phys. Rev. A* **49**, 4110 (1994).
- [28] S. Lloyd, *Phys. Rev. A* **62**, 022108 (2000).
- [29] U. Dorner and P. Zoller, *Phys. Rev. A* **66**, 023816 (2002).
- [30] A. Carmele, J. Kabuss, F. Schulze, S. Reitzenstein, and A. Knorr, *Phys. Rev. Lett.* **110**, 013601 (2013).
- [31] S. M. Hein, F. Schulze, A. Carmele, and A. Knorr, *Phys. Rev. Lett.* **113**, 027401 (2014).
- [32] T. Tufarelli, M. S. Kim, and F. Ciccarello, *Phys. Rev. A* **90**, 012113 (2014).
- [33] Y.-L. L. Fang and H. U. Baranger, *Phys. Rev. A* **91**, 053845 (2015).
- [34] A. L. Grimsmo, *Phys. Rev. Lett.* **115**, 060402 (2015).
- [35] J. Kabuss, D. O. Krimer, S. Rotter, K. Stannigel, A. Knorr, and A. Carmele, *Phys. Rev. A* **92**, 053801 (2015).
- [36] J. Kabuss, F. Katsch, A. Knorr, and A. Carmele, *J. Opt. Soc. Am. B* **33**, C10 (2016).
- [37] H. Chalabi and E. Waks, *Phys. Rev. A* **98**, 063832 (2018).
- [38] N. Német, S. Parkins, A. Knorr, and A. Carmele, *Phys. Rev. A* **99**, 053809 (2019).
- [39] K. Barkemeyer, R. Finsterhölzl, A. Knorr, and A. Carmele, *Adv. Quantum Technol.* **3**, 1900078 (2020).
- [40] K. Sinha, P. Meystre, E. A. Goldschmidt, F. K. Fatemi, S. L. Rolston, and P. Solano, *Phys. Rev. Lett.* **124**, 043603 (2020).
- [41] A. Carmele, N. Nemet, V. Canela, and S. Parkins, *Phys. Rev. Res.* **2**, 013238 (2020).
- [42] U. Schollwöck, *Ann. Phys. (N. Y.)* **326**, 96 (2011).
- [43] H. Pichler and P. Zoller, *Phys. Rev. Lett.* **116**, 093601 (2016).
- [44] P. O. Guimond, M. Pletyukhov, H. Pichler, and P. Zoller, *Quantum Sci. Technol.* **2**, 044012 (2017).
- [45] A. I. Lvovsky, B. C. Sanders, and W. Tittel, *Nat. Photonics* **3**, 706 (2009).
- [46] P. Longo, P. Schmitteckert, and K. Busch, *Phys. Rev. Lett.* **104**, 023602 (2010).
- [47] E. S. Redchenko and V. I. Yudson, *Phys. Rev. A* **90**, 063829 (2014).
- [48] G. Calajó, F. Ciccarello, D. E. Chang, and P. Rabl, *Phys. Rev. A* **93**, 033833 (2016).
- [49] C. W. Hsu, B. Zhen, A. D. Stone, J. D. Joannopoulos, and M. Soljacic, *Nat. Rev. Mater.* **1**, 1 (2016).
- [50] E. Saglamyurek, T. Hrushevskiy, A. Rastogi, K. Heshami, and L. J. LeBlanc, *Nat. Photonics* **12**, 774 (2018).
- [51] F. Dinc, İ. Ercan, and A. M. Brańczyk, *Quantum* **3**, 213 (2019).
- [52] P. Facchi, D. Lonigro, S. Pascazio, F. V. Pepe, and D. Pomarico, *Phys. Rev. A* **100**, 023834 (2019).
- [53] R. Finsterhölzl, M. Katzer, and A. Carmele, *Phys. Rev. B* (to be published).
- [54] T. Tufarelli, F. Ciccarello, and M. S. Kim, *Phys. Rev. A* **87**, 013820 (2013).
- [55] I. C. Hoi, A. F. Kockum, L. Tornberg, A. Pourkabirian, G. Johansson, P. Delsing, and C. M. Wilson, *Nat. Phys.* **11**, 1045 (2015).
- [56] G. Calajó, Y.-L. L. Fang, H. U. Baranger, and F. Ciccarello, *Phys. Rev. Lett.* **122**, 073601 (2019).
- [57] Rodney Loudon, *The Quantum Theory of Light* (Oxford University Press, Oxford, 2000).
- [58] A. Carmele, S. Parkins, and A. Knorr, *Phys. Rev. A* **102**, 033712 (2020).
- [59] M. Fishman, S. R. White, and E. M. Stoudenmire, *The ITensor Software Library for Tensor Network Calculations* (2020), arXiv:2007.14822.
- [60] C. W. Gardiner and M. J. Collett, *Phys. Rev. A* **31**, 3761 (1985).
- [61] C. W. Gardiner and P. Zoller, *Quantum Noise* (Springer, Berlin, 2004).
- [62] P. Domokos, P. Horak, and H. Ritsch, *Phys. Rev. A* **65**, 12 (2002).
- [63] W. Konyk and J. Gea-Banacloche, *Phys. Rev. A* **93**, 063807 (2016).
- [64] E. Schöll, S. H. L. Klapp, and P. Hövel, eds., *Control of Self-Organizing Nonlinear Systems* (Springer, Berlin, 2016).